Electricfield dependence of optical absorption properties in coupled quantum wells and their application to 1.3 m optical modulator

Yimin Huang, Junfu Wang, and Chenhsin Lien

Citation: J. Appl. Phys. **77**, 11 (1995); doi: 10.1063/1.359377

View online: http://dx.doi.org/10.1063/1.359377

View Table of Contents: http://jap.aip.org/resource/1/JAPIAU/v77/i1

Published by the American Institute of Physics.

Electric-field dependence of optical absorption properties in coupled quantum wells and their application to 1.3 μm optical modulator

Yimin Huang
Department of Electronics Engineering and the Institute of Electronics, National Chiao Tung University, Hsinchu, Taiwan 30039, Republic of China

Junfu Wang and Chenhsin Lien[a)]
Department of Electrical Engineering, National Tsing Hua University, Hsinchu, Taiwan 30043, Republic of China

(Received 20 June 1994; accepted for publication 12 September 1994)

A 1.3 μm modulator using light-hole–to-electron interband Stark shift in the lattice-matched AlInAs/GaInAs coupled quantum wells (CQWs) is investigated theoretically. The operation of this device is based on the lowest-energy absorption resonance corresponding to the first light-hole–to–electron transition ($E_{\mathrm{Lh1}} \rightarrow E_{e1}$). The resonant nature of this process results in a sharp absorption peak when the incident photon energy is equal to the energy-level separation. This device utilizes the significant enhancement of the Stark effect on the electronic states and the strong field-dependence transition dipole moments. Under an applied electric field, the energy spacing between E_{Lh1} and E_{e1} changes due to the Stark shift. The contrast ratio can be improved from 8:1 for the symmetric CQW to as high as 20:1 for the proposed asymmetric CQW structure. These contrast ratios are achieved by varying the applied electric field in the 0–70 kV/cm range. This large variation of optical absorption at 1.3 μm is obtained both by the enhanced Stark shift and by varying the overlap between the hole and electron envelope wave functions with an applied electric field and Stark effect for the proposed AlInAs/GaInAs CQW system. © *1995 American Institute of Physics.*

I. INTRODUCTION

Confinement of carriers in a semiconductor quantum well leads to the formation of discrete eigenenergy levels and drastic change of electroabsorption spectrum from the smooth function of bulk material to a series of steps. Additionally, the confinement also increases the binding energy of excitons, resulting in exceptionally clear exciton resonance in various quantum-well structures. The linear exciton electroabsorption of the quantum well has been studied experimentally and very large and sharp optical-absorption resonance has been observed.[1–6] Recently, the study of exciton electroabsorption in quantum-well structures has produced a new class of optoelectronic device with great potential for data processing application. Various information processing system are under development that utilize quantum well *p-i-n* diode light modulator as a primary component.[1–16] The driving force behind these systems is the communication of information on and off the semiconductor chip via a light beam. From the device point of view, the key point for these field-induced switching devices is the capability of modulation of the absorption in the quantum wells by the applied electric field. The quantum confined Stark effect, which generally refers to a shift in the exciton electroabsorption spectrum of a quantum-well device upon the application of an electric field, permits simple electrical control of optical transmission. Because the resulting changes in absorption are large, the modulated light can propagate perpendicularly to the surface of the chip and it is possible to make optical modulators that have desirable electrical properties, operate at room temperature, and show promise of very high speed operation.[12–16] Up to now, the Stark tuning effect has been applied in the related self-electro-optic effect devices (SEEDs)[17,18] to make optical switches, oscillators, and modulators. The tunable photodetectors based on the intersubband Stark shift have also been demonstrated.[19]

Exciton electroabsorption in conjunction with the Stark shift are the most efficient processes for making optical communication intensity modulators. The most important characteristics pertinent to the performance of these modulators are the field-dependence transition dipole moments and the Stark effect. The Stark shift of a square quantum well has been studied and the resulting shift compared to the peak width is rather small for practical device application.[20–22] In order to obtain a large Stark shift at a moderate applied electric field, an increasing amount of interest has been devoted to study more sophisticated quantum-well structures. The coupled quantum well (CQW) structure (shown in Fig. 1) consists of a pair of quantum wells separated by a barrier (about 20–30 Å) narrow enough that considerable interaction occurs between electronic states in these two adjacent wells. In this way, electrons or holes in each well can interact strongly with each other to achieve a large Stark shift. A very strong Stark effect of both intersubband and interband transitions in this quantum-well structure has been predicted theoretically[23–25] and observed experimentally.[26–28] This large Stark shift of energy separation, can be used to tune the resonance absorption for the device, which acts like a voltage tunable filter.[29]

Since the CQW structure does give a very large Stark effect and strong field-dependence transition dipole moments, it is a promising candidate for fabricating optical communication intensity modulators. By employing the lattice-matched AlInAs/GaInAs CQW, a 1.3 μm modulator

[a)]Author to whom correspondence should be addressed.

 0021-8979/95/77(1)/11/6/$6.00

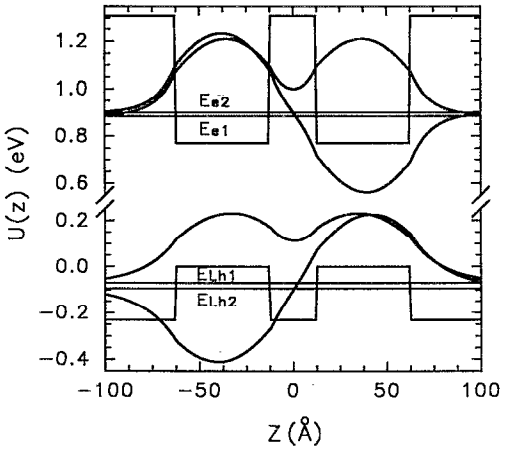

FIG. 1. Schematic band diagram of a symmetric coupled quantum well. The width of each well is 50 Å and the central barrier width is 25 Å. Sub-band energy levels and their associated envelope wave functions are also displayed.

using the light-hole–to–electron interband Stark effect is proposed in this article. The operation of this device is based on the first light-hole–to–electron interband absorption resonance. The resonant nature of this process results in a sharp absorption peak when the incident photon energy is equal to the energy-level separation. This device utilizes both the enhanced Stark effect on the electronic state and the strong field-dependence transition dipole moments. Great modulation of optical absorption at 1.3 μm should be possible for this CQW modulator.

As illustrated in Fig. 1, when two wells are coupled, the coupling of states at each single quantum well through the narrow barrier causes the splitting of each subband into symmetric and antisymmetric states. Application of an electric field can skew the electrons and holes toward opposite sides of the well (as shown in Fig. 2), greatly reducing the overlap between these two symmetric envelope wave functions (resulting in an overall net reduction in the transition dipole moment $\langle\psi_{\mathrm{Lh1}}|z|\psi_{e1}\rangle$). The $E_{\mathrm{Lh1}}\rightarrow E_{e1}$ transition energy also shifts to lower energies with increasing the applied electric field due to the red interband Stark shift. In this way, a large variation of optical absorption at 1.3 μm can be achieved by the Stark shift and by varying the overlap between the hole and electron envelope wave functions with an applied electric field for the proposed CQW system. Since the incident optical radiation on the device is either absorbed or transmitted depending on (1) the energy separation between the confinement energies of the electron and that of the hole in the CQW, and (2) the overlap between envelope wave function of eigenenergy E_{Lh1} and that of E_{e1}, the desired modulation of 1.3 μm photon energy can be achieved by adjusting the energy spacing and the transition dipole moment between these two subbands under an appropriate electric field. Based on theoretical calculations, the contrast ratio of 8:1 is predicted for the proposed symmetric CQW. This contrast ratio is achieved by varying the applied electric field in the 0 to 70 kV/cm.

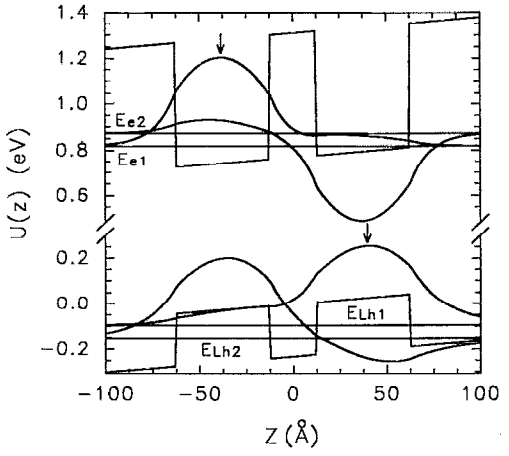

FIG. 2. Electronic potential energy profile for the symmetric CQW structure under the applied electric field of 70 kV/cm. The envelope wave function of E_{Lh1} shifts to the right-hand-side well and that of the E_{e1} to the left-hand-side, thus reducing the overlap between these two envelope wave functions.

The symmetric CQW does give a large Stark effect and a strong field-dependence transition dipole moment, however, this symmetric structure has one drawback as a competitive candidate for high contrast ratio of 1.3 μm modulator due to the field-induced absorption such as $E_{\mathrm{Lh1}}\rightarrow E_{e2}$ and $E_{\mathrm{Lh2}}\rightarrow E_{e1}$ exciton absorption, which is located close to the 1.3 μm spectral region. In practice, the exciton absorption of $E_{\mathrm{Lh1}}\rightarrow E_{e2}$ and $E_{\mathrm{Lh2}}\rightarrow E_{e1}$ do limit the minimum attainable absorption in the presence of the applied electric field. As a result, the contrast ratio cannot be improved for the symmetric CQW. For the asymmetric CQW, the energy spacing for the $E_{\mathrm{Lh1}}\rightarrow E_{e2}$ and $E_{\mathrm{Lh2}}\rightarrow E_{e1}$ transitions can be designed to be much larger than that of the $E_{\mathrm{Lh1}}\rightarrow E_{e1}$ transition due to the quantum size effect. In this way, by moving the absorption due to the $E_{\mathrm{Lh1}}\rightarrow E_{e2}$ and $E_{\mathrm{Lh2}}\rightarrow E_{e1}$ transitions away from the 1.3 μm spectral region, an asymmetric CQW modulator with very high contrast ratio can be obtained. A contrast ratio as high as 20:1 is achieved as the electric field varies from 0 to 70 kV/cm.

This article is organized into four sections: In Sec. II, a theoretical basis for the calculations is laid, and in Sec. III graphs from numerical calculations are presented along with discussions.

II. THEORY AND FORMALISM

In this section, the numerical method to evaluate the eigenenergies and the envelope wave functions is described for the CQW structure under the influence of an applied electric field. The results of the derivation are essential to understand the physical properties of electrons and holes in these quantum-well structures and the characteristics of the modulator employing these quantum-well structures.

The CQW generally refers to a structure where a thin barrier layer is sandwiched between two wells. Since this barrier is very thin, there is an appreciable interaction among electronic states in these two wells. Depending on the width difference between these two wells the CQW systems are divided into two categories: symmetric CQWs (Fig. 1) and asymmetric CQWs (Fig. 3). The conduction-band eigenener-

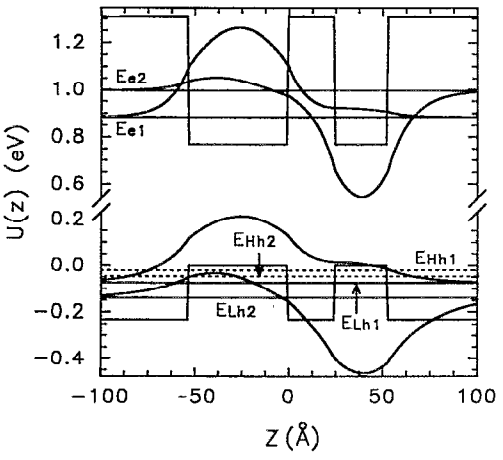

FIG. 3. Schematic band diagram of an asymmetric coupled quantum well. The width of these two wells is 53 and 28 Å, respectively. Subband energy levels and their associated envelope wave functions are also displayed.

gies of the one-dimensional finite potential well can be found by solving the time-independent Schrödinger equation,

$$H_e\psi_e=\left(-\frac{\hbar^2}{2m_e^*}\frac{\partial^2}{\partial z^2}+U_e(z)+eFz\right)\psi_e=E_e\psi_e, \qquad (1)$$

where $U_e(z)$ is the rectangular quantum-well potential for electrons due to the conduction-band discontinuity, m_e^* is the effective mass of electrons in conduction band, F is the applied electric field, and $\hbar=h/2\pi$, where h is the Plank's constant. E_e and ψ_e represent the energy eigenvalue and eigenfunction of the electron in the conduction band. At the AlInAs/GaInAs interface the electronic wave function and its first derivative ψ_e'/m_e^* are assumed to satisfy the continuity condition. In the presence of a static electric field, although there are no bound states in the finite depth quantum well, there still exist some quasibound states in the well. Here, the staircase approximation of the transfer-matrix formalism is used to calculate the envelope wave functions of the quasibound state of the CQW system under the external electric field.[19] The only assumption needed is that the envelope wave function goes to zero at a position far away from the quantum well.

The calculation of transition energies in a complete quantum-well system involves calculation of both the valence- and conduction-band eigenenergies. The conduction-band eigenenergies calculation proceeds as described above. However, to insure computational simplicity, several assumptions have been made in modeling the valence band. The heavy and light holes were treated separately and band-mixing effects between the heavy and light hole were not included.[1,27] With these assumptions, the valence band can be solved computationally as if it was a conduction band well under the opposite sign of field (incorporating appropriate changes in the values of the effective mass and depth of the quantum-well structure).

The energy for a light-hole exciton absorption can be expressed as[12]

$$E_{mn}^{(ex)}=E_g+E_{\mathrm{Lh}m}+E_{en}-B, \qquad (2)$$

where E_g is the energy gap of the GaInAs layer, B is the binding energy of the exciton, and $E_{\mathrm{Lh}m}$ and E_{en} are the mth and nth confinement energies of the hole and electron subbands, respectively. In this article only the perpendicular polarization of the optical signal is considered and the heavy holes contributed to the exciton absorption are not be considered here. Note that, in the perpendicular polarization, only the light-hole transitions exist because selection rules prohibit any heavy-hole transition.[1] The variation of E_g under a static field is rather small, because it is associated with a modification of the unit-cell wave function, and can be neglected.[12] Conversely the variation of the confinement energies $E_{\mathrm{Lh}m}$ and E_{en} result from the modification of the envelope wave functions within the CQW are very sensitive to the applied electric field. Consequently, a large changes in the exciton absorption can be achieved with the applied electric field. The binding energy B is assumed to be 10 meV.[10]

The absorption coefficient for the band-to-band transition is given by[30]

$$\alpha(\hbar\omega)=\frac{4\pi^2e^2\hbar}{\eta cm^2}\left(\frac{1}{\hbar\omega}\right)\sum_{k_\parallel}\sum_{n,m}|\hat{a}\cdot\mathbf{p}_{nm}(k_\parallel)|^2 \times\delta[E_m^h(k_\parallel)-E_n^e(k_\parallel)+\hbar\omega], \qquad (3)$$

where η is the index of the refraction, $\hat{a}$ is polarization vector of the radiation, m, n are the hole and electron subband indexes, and c is the speed of light in vacuum. The optical matrix element is given by

$$\mathbf{p}_{nm}(k_\parallel)=\langle\Psi_m^h(k_\parallel)|\mathbf{P}|\Psi_n^e(k_\parallel)\rangle, \qquad (4)$$

where $\Psi_m^h(k_\parallel)$ and $\Psi_n^e(k_\parallel)$ are the hole and electron wave functions. The absorption due to the exciton is then added to the band-to-band absorption. The exciton absorption coefficient is given by[30]

$$\alpha_{\mathrm{ex}}(\hbar\omega)=\frac{4\pi^2e^2\hbar}{\eta cmW}\left(\frac{1}{\hbar\omega}\right)\times\left|\sum_{k_\parallel}G_{nm}(k_\parallel)\hat{a}\cdot\mathbf{p}_{nm}(k_\parallel)\right|^2 \times\delta(\hbar\omega-E_{mn}^{\mathrm{ex}}), \qquad (5)$$

where $G_{nm}(k_\parallel)$ is the Fourier transform of the exciton wave function. To account for the broadening mechanisms, the delta functions in Eqs. (3) and (5) are replaced by a Lorentzian function, i.e., $\delta(\hbar\omega-E)$ by

$$\frac{1}{\pi}\frac{\hbar/\tau}{(E-\hbar\omega)^2+(\hbar/\tau)^2},$$

where τ is the dephasing time.

III. RESULTS AND DISCUSSIONS

The mathematical method to find the conduction- and valence-band eigenenergies for various CQW structures with applied electric field have been developed in Sec. II. The theories for the absorption coefficient have been also described. Based on these theories, numerical results and discussions are presented in this section. All the numerical calculation done in this article is based on the following parameters unless otherwise stated: the central barrier width is 25 Å, $T=77$ K, and all of the dephasing time τ are as-

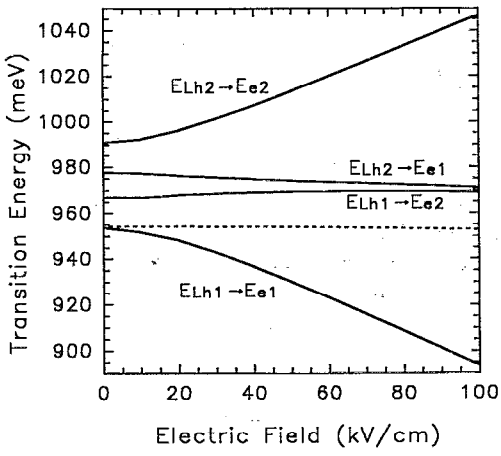

FIG. 4. Relation of the light-hole exciton transition energies as a function of the applied electric field for the symmetric CQW. The dashed line indicates the first light-hole–to–electron transition energy for a single quantum well with a well width of 54 Å.

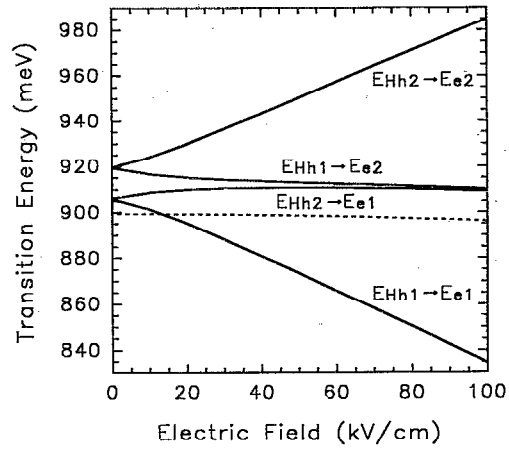

FIG. 5. Relation of the heavy-hole exciton transition energies as a function of the applied electric field for the symmetric CQW. The dashed line indicates the first heavy-hole–to–electron transition energy for a single quantum well with a well width of 54 Å.

sumed to have the same values of 0.14 ps (corresponding to a linewidth of about 15 meV). The conduction-band-gap discontinuity and effective mass of carriers for AlInAs/GaInAs material system used here are adopted from Ref. 31.

A. Symmetric CQW systems

The band diagram and envelope wave functions of a symmetric CQW, consisting of a pair of 50 Å $Ga_{0.47}In_{0.53}As$ quantum wells separated by an $Al_{0.48}In_{0.52}As$ barrier surrounded by $Al_{0.48}In_{0.52}As$ outer barrier, without applied electric field, are shown in Fig. 1. In absence of the applied electric field, the CQW structure has well-defined symmetry and the coupling of states at each single quantum well through narrow barrier causes the splitting of each subband into symmetric and antisymmetric states. For example, the ground-state subband E_{Lh1} of the valence band for an isolated quantum well splits into E_{Lh1} (symmetric state) and E_{Lh2} (antisymmetric state) for CQW. The relation of the light-hole exciton transition energy $E_{\mathrm{Lh}m}\rightarrow E_{en}$ as a function of the applied electric field for the symmetric CQW (solid line) and an $Al_{0.48}In_{0.52}As/Ga_{0.47}In_{0.53}As$ single quantum well with a width of 54 Å (dashed line) are shown in Fig. 4. The positive direction of the applied electric field is defined as from left- to right-hand side (i.e., positive z direction). As expected, a large variation of exciton transition energies arises due to the application of an electric field. Thus, the symmetric CQWs do have a large Stark effect as compared to the small Stark shifts of the single-quantum-well structure (dashed line). The eigenenergies and the envelope wave functions of the symmetric CQW under an applied electric field of 70 kV/cm are shown in Fig. 2. By comparing the eigenenergies on Fig. 1 to that of Fig. 2, the advantage of the coupled effect of the symmetric CQW becomes evident. Note that the symmetric and antisymmetric states show opposite shifting trends when an external field is applied. It is clear that the electric field perpendicular to the CQW pulls the electrons and hole toward the opposite side of the well resulting in an overall net reduction (increase) in the exciton transition $E_{\mathrm{Lh1}}\rightarrow E_{e1}$ ($E_{\mathrm{Lh2}}\rightarrow E_{e2}$) and a corresponding Stark shift in the exciton absorption. The relation of the heavy-hole exciton transition energy $E_{\mathrm{Hh}m}\rightarrow E_{en}$ as a function of the applied electric field for the symmetric CQW and a single quantum well are also shown in Fig. 5 for comparison. Similar results of the field-induced shift in heavy-hole exciton transition energies should also be expected in CQWs. Thus, the symmetric CQWs do give an enhanced Stark effect.

The absorption coefficient can be evaluated by using Eqs. (3) and (5). The exciton absorption spectrum for the symmetric CQW at $F=0$ (solid line) and $F=70$ kV/cm (dashed line) is shown in Fig. 6. Here, only the light-hole exciton absorption ($E_{\mathrm{Lh}n}\rightarrow E_{em}$) is plotted. It is evident that the absorption coefficient for the first exciton transition $E_{\mathrm{Lh1}}\rightarrow E_{e1}$ drops sharply from $F=0$ to 70 kV/cm due to the reduction of the overlap between envelope wave functions of these eigenenergy states. The resulting relation between the transition dipole moment and the applied electric field for the

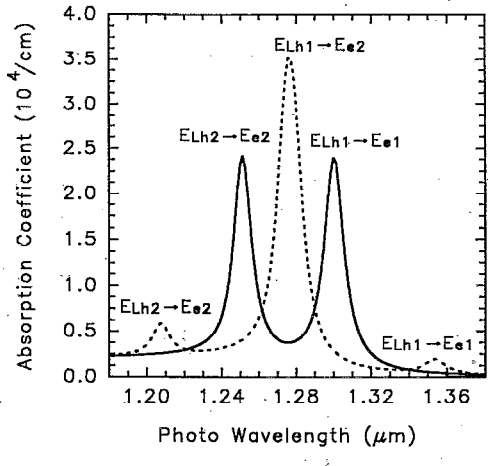

FIG. 6. Calculated light-hole exciton absorption coefficient as a function of the photon wavelength for the symmetric coupled quantum well at $F=0$ (solid line) and $F=70$ kV/cm (dashed line).

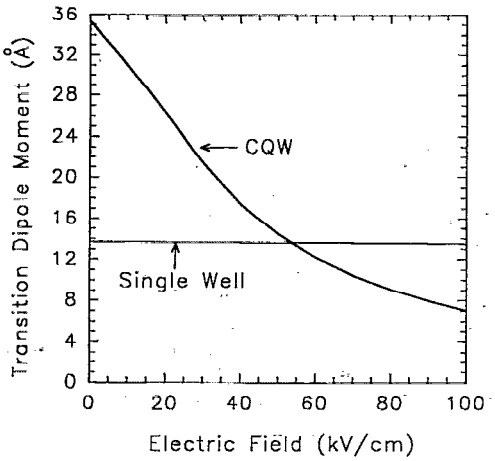

FIG. 7. Calculated first light-hole–to–electron transition dipole moment as a function of the applied electric field for the symmetric coupled quantum well and a single quantum well.

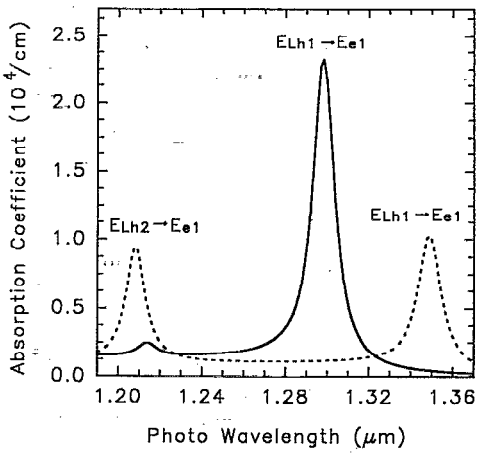

FIG. 8. Calculated light-hole exciton absorption coefficient as a function of the photon wavelength for the asymmetric coupled quantum well at $F=0$ (solid line) and $F=70$ kV/cm (dashed line).

$E_{\mathrm{Lh1}}\rightarrow E_{e1}$ transition in symmetric CQW and in single quantum well is shown in Fig. 7. As can be seen that the transition dipole moment for the CQW decreases sharply as the applied electric field is increased. From Figs. 1 and 2, it is clear that the envelope wave functions of the E_{Lh1} and that of the E_{e1} tend to shift oppositely in the presence of an applied electric field and a lower transition dipole moment is expected due to the decrease of overlap between envelope wave functions. As a result, a lower absorption coefficient is expected for CQW under the higher electric field. As for the single quantum well, the dipole moment is almost unchanged in the presence of the applied electric field. Notice that the dipole moment element can be more sensitive to the applied electric field for the single quantum well with a larger well width; however, the field-dependent transition dipole moment is much weaker as compared to that of the CQW structures. From Fig. 6 it is evident that the peak absorption of the $E_{\mathrm{Lh1}}\rightarrow E_{e1}$ is shifted to longer wavelength as the applied electric field is increased. The shift in the exciton absorption can be understand in terms of the Stark shift in the confinement energies of E_{Lh1} and E_{e1}. The symmetric CQW does give a large Stark effect and the strong field dependent transition dipole moment. The contrast ratio of 8:1 is predicted for the symmetric CQW modulator. This contrast ratio is achieved as the applied electric field is changed from 0 to 70 kV/cm.

B. Asymmetric CQW systems

Although the symmetric CQW has both the large Stark shift and the strong field-dependent transition dipole moment, still its contrast ratio cannot be improved very much beyond 8:1. This relatively low contrast ratio hinders the symmetric CQW as a competitive candidate for high-contrast-ratio 1.3 μm modulator application. This drawback is due to the absorption of those field-induced transitions such as $E_{\mathrm{Lh1}}\rightarrow E_{e2}$ and $E_{\mathrm{Lh2}}\rightarrow E_{e1}$. For symmetric CQW, absorption peaks due to these transitions locate rather close to the 1.3 μm spectral region. Although these transitions are forbidden in the absence of the applied electric field because the dipole moment elements $\langle\psi_{\mathrm{Lh1}}|z|\psi_{e2}\rangle$ and $\langle\psi_{\mathrm{Lh2}}|z|\psi_{e1}\rangle$ vanish for the symmetric system, still these transition can be activated by breaking the symmetric property with an applied electric field. It is clear from Fig. 6 that the absorption of $E_{\mathrm{Lh1}}\rightarrow E_{e2}$ and $E_{\mathrm{Lh2}}\rightarrow E_{e1}$ dominate the absorption spectrum at $F=70$ kV/cm and do in practice limit the minimum attainable absorption in the presence of the applied electric field. As a result, the contrast ratio cannot be improved very much with this symmetric CQW structure. In contrast, the asymmetric CQW (as shown in Fig. 3) can be designed to give a very large contrast ratio by forcing the energy spacing of both the $E_{\mathrm{Lh1}}\rightarrow E_{e2}$ and $E_{\mathrm{Lh2}}\rightarrow E_{e1}$ transitions much larger than that of the $E_{\mathrm{Lh1}}\rightarrow E_{e1}$ transition. For the asymmetric CQW, the eigenenergy of the ground-state subband of the whole CQW is roughly equal to the eigenenergy of the ground-state subband of the wide well and the eigenenergy of the first-excited-state subband of the whole CQW is approximately equal to the eigenenergy of the ground-state subband of the narrow well. By choosing an appropriate width of the narrow well, the energy spacing of both the $E_{\mathrm{Lh1}}\rightarrow E_{e2}$ and $E_{\mathrm{Lh2}}\rightarrow E_{e1}$ transitions can be made much larger than that of the $E_{\mathrm{Lh1}}\rightarrow E_{e1}$ transition due to the quantum size effect. In this way, the absorption due to $E_{\mathrm{Lh1}}\rightarrow E_{e2}$ and $E_{\mathrm{Lh2}}\rightarrow E_{e1}$ transitions are removed from the 1.3 μm spectral region and an asymmetric CQW modulator with high contrast ratio can be designed.

The exciton absorption spectra for the asymmetric CQW at $F=0$ (solid line) and $F=70$ kV/cm (dashed line) are shown in Fig. 8. From this result, it can be seen that the modulation depth of optical switching devices based on the quantum-confined Stark effect can be enhanced by using an asymmetric CQW structure. The contrast ratio as high as 20:1 can be achieved as the electric field varies from 0 to 70 kV/cm. Moreover, by adjusting the width of each well and barrier more flexibility of device engineering may be achieved.

IV. CONCLUSIONS

Conventional multi-quantum-well structures show a weak field-dependent transition dipole moment of the exci-

ton transition and no evidence of the Stark shift. Thus, it is not a promising candidate for optical communication intensity modulators with high contrast ratio. Coupled quantum wells with a large Stark effect and strong field-dependent transition dipole moment can be used to fabricate a modulator with a greater modulation depth. The 1.3 μm AlInAs/GaInAs symmetric CQW and asymmetric CQW modulators with contrast ratio of 8:1 and 20:1, respectively, have been proposed in this article. These devices utilize the significant enhancement of the Stark effect and strong field-dependent transition dipole moment. A large variation of optical absorption at 1.3 μm under an applied electric field can be obtained for these CQW structures. These CQW modulators are ideal for the optical communication intensity modulators. By using a smaller energy band-gap material, such as strained AlInAs/$Ga_xIn_{1-x}As$ with $x<0.47$ grown on an InP substrate, a modulator for the application in long-distance 1.55 μm fiber communication can also be designed.

ACKNOWLEDGMENT

This research was supported in part by the National Science Council of Republic of China under Contract No. NSC-80-0417-E007-05.

[1] M. N. Isiam, R. L. Hillman, D. A. B. Miller, D. S. Chemla, A. C. Gossard, and J. H. English, Appl. Phys. Lett. **50**, 1098 (1987).
[2] G. D. Boyd, D. A. B. Miller, D. S. Chemla, S. L. McCall, A. C. Gossard, and J. H. English, Appl. Phys. Lett. **50**, 1119 (1987).
[3] C. Thirstrup, Appl. Phys. Lett. **61**, 2641 (1992).
[4] J. E. Cunningham, K. W. Goossen, M. Williams, and W. Y. Jan, Appl. Phys. Lett. **60**, 727 (1992).
[5] K. W. Goossen, J. E. Cunningham, and W. Y. Jan, Appl. Phys. Lett. **64**, 1071 (1994).
[6] D. J. Goodwill, A. C. Walker, C. R. Stanley, M. C. Holland, and M. McElhinney, Appl. Phys. Lett. **64**, 1192 (1994).
[7] S. S. Lee, Y. S. Kim, R. V. Ramaswamy, and V. S. Sundaram, Appl. Phys. Lett. **55**, 1865 (1989).
[8] K.-K. Law, R. H. Yan, J. L. Merz, and L. A. Coldren, Appl. Phys. Lett. **56**, 1886 (1990).
[9] K. Hu, L. Chen, A. Madhukar, P. Chen, C. Kyriakakis, Z. Karim, and A. R. Tanguay, Jr., Appl. Phys. Lett. **59**, 1664 (1991).
[10] T. A. Vang, G. W. Taylor, P. A. Evaldsson, and P. Cooke, Appl. Phys. Lett. **61**, 2464 (1992).
[11] T. Tutken, B. J. Hawdon, M. Zimmermann, I. Queisser, A. Hangleiter, V. Harle, and F. Scholz, Appl. Phys. Lett. **64**, 403 (1994).
[12] T. H. Wood, C. A. Burrus, D. A. B. Miller, D. S. Chemla, T. C. Damen, A. C. Gossard, and W. Wiegmann, Appl. Phys. Lett. **44**, 16 (1984).
[13] J. Nees, S. Williamson, and G. Mourou, Appl. Phys. Lett. **54**, 1962 (1989).
[14] D. Mahgerefteh, C.-M. Yang, L. Chen, K. Hu, W. Chen, E. Garmire, and A. Madhukar, Appl. Phys. Lett. **61**, 2592 (1992).
[15] F. Devaus, E. Bigan, M. Allovon, J.-C. Harmand, F. Huet, M. Carre, and J. Landreau, Appl. Phys. **61**, 2773 (1992).
[16] N. M. Froberg, A. M. Johnson, K. W. Goossen, J. E. Cunningham, M. B. Santos, W. Y. Jan, T. H. Wood, and C. A. Burrus, Jr., Appl. Phys. Lett. **64**, 1705 (1994).
[17] L. Chen, K. Hu, R. M. Kapre, and A. Madhukar, Appl. Phys. Lett. **64**, 422 (1992).
[18] A. L. Lentine, H. S. Hinton, D. A. B. Miller, J. E. Henry, J. E. Cunningham, and L. M. F. Chirovsky, Appl. Phys. Lett. **52**, 424 (1988).
[19] Y. Huang, C. Lien, and T.-F. Lei, J. Appl. Phys. **74**, 2598 (1993).
[20] K. W. Goossen, J. E. Cunningham, M. B. Santos, and W. Y. Jan, Appl. Phys. Lett. **62**, 3229 (1993).
[21] S. R. Parihar, S. A. Lyon, M. Santos, and M. Shayegan, Appl. Phys. Lett. **55**, 2417 (1989).
[22] A. Harwit and J. S. Harris, Jr., Appl. Phys. Lett. **50**, 685 (1987).
[23] I. Galbraith and G. Duggan, Phys. Rev. B **40**, 5515 (1989).
[24] D. Ahn, IEEE J. Quantum Electron. **QE-25**, 2260 (1989).
[25] W. Q. Chen, S. M. Wang, and T. G. Andersson, IEEE Electron Device Lett. **EDL-14**, 286 (1993).
[26] C. Sirtori, F. Capasso, D. L. Sivco, A. L. Hutchinson, and A. Y. Cho, Appl. Phys. Lett. **60**, 151 (1992).
[27] K. J. Kuhn, C. Juang, and R. B. Darling, J. Appl. Phys. **69**, 3135 (1991).
[28] J. Faist, F. Capasso, C. Sirtori, D. Sivco, A. L. Hutchinson, S.-N. G. Chu, and A. Y. Cho, Appl. Phys. Lett. **64**, 1144 (1994).
[29] R. P. G. Karunasiri, Y. J. Mii, and K. L. Wang, IEEE Electron Device Lett. **EDL-11**, 227 (1990).
[30] S. C. Hong, M. Jaffe, and J. Singh, IEEE J. Quantum Electron. **QE-23**, 2181 (1987).
[31] B. F. Levine, A. Y. Cho, J. Walker, R. J. Malik, D. A. Kleinman, and D. L. Sivco, Appl. Phys. Lett. **52**, 1481 (1988).